NATIONAL ADVISORY COMMITTEE FOR AERONAUTICS

REPORT 1162

LIFT DEVELOPED ON UNRESTRAINED RECTANGULAR WINGS ENTERING GUSTS AT SUBSONIC AND SUPERSONIC SPEEDS

By HARVARD LOMAX

1954

For sale by the Superintendent of Documents, U. S. Government Printing Office, Washington 25, D. C. Yearly subscription, $10.00; foreign, $11.25; single copy price varies according to size - - - - - - - - - - Price 20 cents

REPORT 1162

LIFT DEVELOPED ON UNRESTRAINED RECTANGULAR WINGS ENTERING GUSTS AT SUBSONIC AND SUPERSONIC SPEEDS

By HARVARD LOMAX

Ames Aeronautical Laboratory
Moffett Field, Calif.

National Advisory Committee for Aeronautics

Headquarters, 1724 F Street NW., Washington 25, D. C.

Created by act of Congress approved March 3, 1915, for the supervision and direction of the scientific study of the problems of flight (U. S. Code, title 50, sec. 151). Its membership was increased from 12 to 15 by act approved March 2, 1929, and to 17 by act approved May 25, 1948. The members are appointed by the President, and serve as such without compensation.

Conduct, under unified control, for all agencies, of scientific research on the fundamental problems of flight

REPORT 1162

LIFT DEVELOPED ON UNRESTRAINED RECTANGULAR WINGS ENTERING GUSTS AT SUBSONIC AND SUPERSONIC SPEEDS [1]

By Harvard Lomax

SUMMARY

The object of this report is to provide an estimate, based on theoretical calculations, of the forces induced on a wing that is flying at a constant forward speed and suddenly enters a vertical gust. The calculations illustrate the effects of Mach number (from 0 to 2) and aspect ratio (2 to ∞), and solutions are given by means of which the response to gusts having arbitrary distributions of velocity can be calculated. The effects of pitching and wing bending are neglected and only wings of rectangular plan form are considered. Specific results are presented for sharp-edged and triangular gusts and various wing-air density ratios.

INTRODUCTION

Studies of the gust-response problem for restrained wings (wings of infinite mass) entering sharp-edged gusts at supersonic speeds are already well advanced. Miles, Strang, Biot, and Heaslet and Lomax (refs. 1, 2, 3, and 4) presented solutions to such problems for two-dimensional wings; Miles and Goodman (refs. 5 and 6) presented solutions for rectangular wings having tip Mach cones that do not intersect the opposite edge. Miles and Strang (refs. 7 and 8) gave results for a triangular wing with supersonic edges. Theoretical studies restricted to incompressible flow fields contain the classical solutions due to Wagner (ref. 9), Kussner (ref. 10), and von Kármán and Sears (ref. 11), the former containing the solution for the indicial lift on a two-dimensional sinking wing and the latter two containing the solution for the lift on a restrained two-dimensional wing entering a sharp-edged gust. The extension of these studies to include the gust response for wings of finite aspect ratio has been carried out by Jones (ref. 12). Later, further extensions to include the effects of gust shape as well as aspect ratio have been made by Zbrozek (ref. 13) and Bisplinghoff, Isakson, and O'Brien (ref. 14).

The purpose of the present report is twofold: first, to present solutions for a two-dimensional restrained wing entering a sharp-edged gust at sonic and subsonic Mach numbers (specifically, Mach numbers equal to 1.0, 0.8, and 0.5); and second, to use these results together with those mentioned above to estimate the effect of wing aspect ratio and airplane mass on the lift response for airplanes flying at various speeds through the Mach number range from 0 to 2 and penetrating both triangular and sharp-edged gusts.

A list of symbols is given in the appendix.

ANALYSIS

THE EQUATION OF MOTION

If induced pitching moments are neglected, the motion of a rigid wing disturbed from its equilibrium position by arbitrary external lifting forces is governed by Newton's second law. Thus, if w is the vertical velocity of the wing and m its mass, we can write

$$m\frac{dw}{dt'}=\sum \text{forces} \tag{1}$$

where the forces to be summed are the aerodynamic ones due to the gust velocity and the motion of the wing from its position of equilibrium.

First, consider the force that results from a small vertical motion of the wing. Suppose the wing has been flying in steady level flight at a constant speed U_0 up to a time $t'=0$. Fix an xyz coordinate system in space (z positive upward) such that at $t'=0$ the y axis lies along, and the origin on, the wing leading edge and, further, such that the wing is moving in the negative x direction. For $t'>0$ the wing moves away from these coordinates, continuing forward at the constant speed U_0 along the negative x axis, and now also moving downward at a constant rate $-w=U_0\alpha$. The transient lifting force on the wing induced by such a maneuver shall be referred to as the indicial lift (positive upward) and designated in coefficient form by the symbols c_{l_α} or C_{L_α} for section or total lift values, respectively.

Given the indicial lift coefficient, one can show by using the prinicples of superposition that the lift due to an arbitrary variation of angle of attack caused by the vertical velocity of the wing can be determined from the relation

$$L(t')=-\frac{qS}{U_0}\frac{d}{dt'}\int_0^{t'} C_{L_\alpha}(t'-t_1')\,w(t_1')\,dt_1' \tag{2a}$$

Next, consider the force that is induced on a wing penetrating a sharp-edged gust having a uniform upward velocity w_0. If the wing is restrained so that it can move neither upward nor downward (corresponding in flight to the limiting case of infinite wing mass), the section or total lift coefficients induced by a unit value of w_0/U_0 will be designated c_{l_g} or C_{L_g}, respectively. Figure 1 illustrates the differences between the boundary conditions for, and the initial variations of c_{l_α} and c_{l_g} for a two-dimensional wing traveling at a subsonic speed.

[1] Supersedes NACA TN 2925, "Lift Developed on Unrestrained Rectangular Wings Entering Gusts at Subsonic and Supersonic Speeds" by Harvard Lomax, 1953.

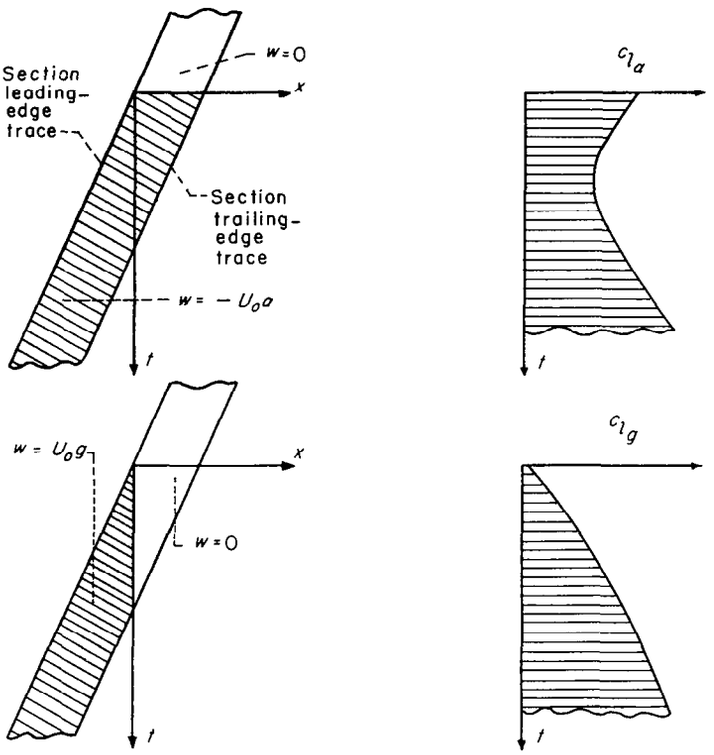

FIGURE 1.—Boundary conditions and initial variations of c_{l_α} and c_{l_g}.

Given a value of C_{L_g}, one obtains the lift on a restrained wing flying into a gust having an arbitrary vertical velocity distribution, $w_a(t')$, by the relation

$$L(t')=\frac{qS}{U_0}\frac{d}{dt'}\int_0^{t'} C_{L_g}(t'-t_1')\,w_a(t_1')\,dt_1' \tag{2b}$$

Substituting equations (2a) and (2b) into equation (1), one finds the expression for the vertical motion of an unrestrained wing flying into a gust; thus,

$$m\frac{dw}{dt'}=-\frac{qS}{U_0}\frac{d}{dt'}\int_0^{t'} C_{L_\alpha}(t'-t_1')\,w(t_1')\,dt_1'+\frac{qS}{U_0}\frac{d}{dt'}\int_0^{t'} C_{L_g}(t'-t_1')\,w_a(t_1')\,dt_1' \tag{3a}$$

Since $w_a(t_1')$ is assumed to be given, equation (3a) is an integral equation—in terms of $w(t')$—of the second kind with a variable upper limit. It is convenient first to study equation (3a) when the gust is a step function (sharp-edged gust). For this case $w_a(t_1')$ becomes a constant w_0, say, and equation (3a) reduces to

$$m\frac{dw}{dt'}=-\frac{qS}{U_0}\frac{d}{dt'}\int_0^{t'} C_{L_\alpha}(t'-t_1')\,w(t_1')\,dt_1'+\frac{qSw_0}{U_0}C_{L_g}(t') \tag{3b}$$

The solution to equation (3b) can be used to find the induced force on an unrestrained wing entering a gust of arbitrary structure. Methods for solving the integral equation and applying its solution will be developed in the subsequent sections.

INDICIAL LIFT ON A SINKING WING

The analysis involved in calculating the indicial lift force on the wing is based on the assumptions that underlie linearized, thin-airfoil wing theory in general. Mathematically, these assumptions imply that the governing partial differential equation of the flow field is the three-dimensional wave equation. In terms of the velocity potential φ and for an axial system fixed relative to the still air at infinity, the wave equation can be written

$$\varphi_{xx}+\varphi_{yy}+\varphi_{zz}=\varphi_{tt} \tag{4}$$

where t is the product of the speed of sound a_0 and the time t'. For a wing moving in the $z=0$ plane, the boundary conditions are that φ is continuous everywhere except across the wing and its vortex wake, $(\varphi_z)_{z=0}$ is a constant over the region bounded by the wing plan form at any given time, and all velocities vanish outside the starting wave envelope.

All values of C_{L_α} and c_{l_α} used herein have been presented in previously published reports. The indicial lift on a sinking rectangular wing traveling at supersonic speeds has been presented by Miles (ref. 5). As the aspect ratio tends to infinity, this solution approaches that for the two-dimensional case given in references 1, 2, 3, and 4. At sonic and subsonic speeds, results for a two-dimensional wing are available for Mach numbers equal to 1.0, 0.8, and 0.5 (ref. 15) and for the incompressible case (ref. 16). Finally, the indicial lift on sinking wings of finite aspect ratio in incompressible flow is presented in reference 12. Curves showing the effect of Mach number on the two-dimensional values are presented in figure 2 (a), and the effect of aspect ratio at supersonic speeds is indicated in figure 2 (b). Tabular values for the two-dimensional wing flying at Mach numbers equal to 0.5 and 0.8 are given in tables I and II, respectively.

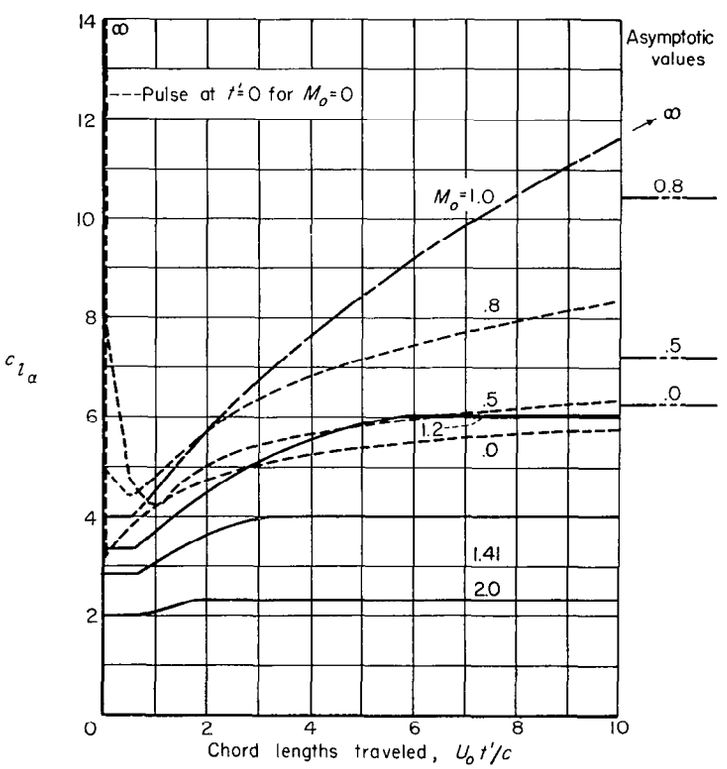

(a) Two-dimensional wing for several Mach numbers.

FIGURE 2.—Variation of indicial lift response with chord lengths traveled.

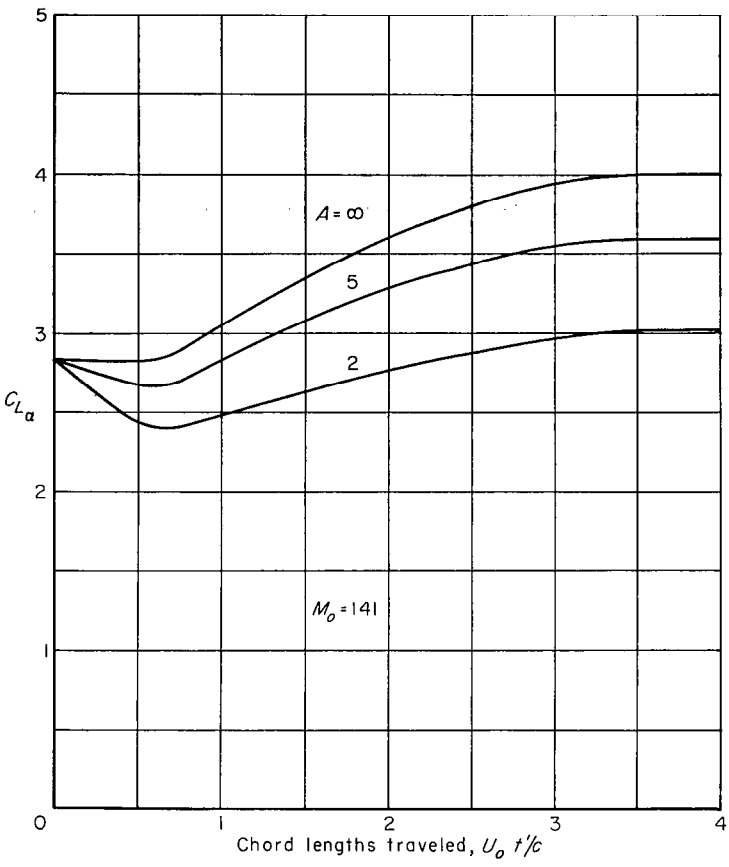

(b) Rectangular wings of aspect ratios 2, 5, and ∞.
FIGURE 2.—Concluded.

RESPONSE OF A RESTRAINED WING TO A SHARP-EDGED GUST

Load distribution.—The lift induced on a restrained wing penetrating a sharp-edged gust can also be determined by solving equation (4) subject to the proper boundary conditions.[2] For a wing moving in the $z=0$ plane, these conditions are similar to those given for the indicial lift on a sinking wing in that all velocities vanish outside the starting wave envelope and φ is continuous everywhere except across the wing and its vortex wake, but differ from the indicial case in that $(\varphi_z)_{z=0}$ is a constant only over the portion of the wing plan form that has penetrated the gust, being zero over the remaining portion (see fig. 1). This problem has been solved for a rectangular wing traveling at supersonic speeds by Miles (ref. 5) and, again, as the aspect ratio tends to infinity, this solution approaches that for the two-dimensional case given in references 1, 2, 3, and 4. Two-dimensional wings flying at the speed of sound and two- and three-dimensional wings flying in an incompressible medium have also been considered (refs. 4, 16, and 12, respectively).

The problem of finding the two-dimensional gust response at subsonic speeds can be solved by the same method that was used in reference 15 to find the two-dimensional subsonic indicial response. For these cases equation (4) reduces to

$$\varphi_{xx}+\varphi_{zz}=\varphi_{tt} \tag{5}$$

[2] It is interesting to note that the gust lift function c_{l_g} can be related to the indicial response following a step variation of angle of attack under quite general conditions by the reciprocal theorems given in reference 17.

and the boundary conditions for a section in the xt plane are indicated in figure 3.

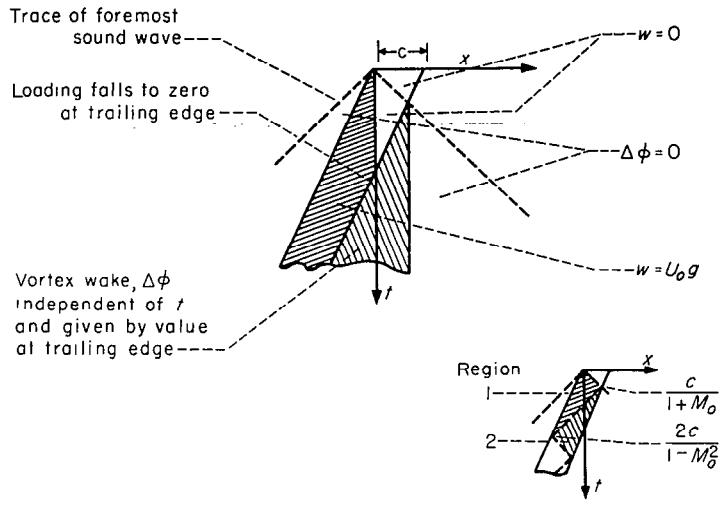

FIGURE 3.—Boundary values for c_{l_g}.

The solutions obtained for the load coefficient over regions 1 and 2 shown in figure 3 can be written (details of the analysis are omitted):
For region 1

$$\frac{\Delta p}{qg}=\frac{\Delta p}{q\left(\frac{w_0}{U_0}\right)}=\frac{8}{\pi(1+M_0)}\sqrt{\frac{M_0(t-x)}{x+M_0t}} \tag{6a}$$

For region 2

$$\frac{\Delta p}{qg}=\frac{8}{\pi(1+M_0)}\left\{\sqrt{\frac{M_0(t-x)}{x+M_0t}}+\frac{2}{\pi}\sqrt{M_0(t-x)(c-x-M_0t)}\right.$$
$$\left.\left[\frac{2K}{\sqrt{(t^2-x^2)(1-M_0^2)}}-\frac{EF'(\psi)+KE'(\psi)-KF'(\psi)}{\sqrt{(x+M_0t)(c-x-M_0t)}}\right]\right\} \tag{6b}$$

The symbols E, K, $E'(\psi)$, and $F'(\psi)$ are elliptic integrals defined in the appendix, their modulus k being given by

$$k=\sqrt{\frac{(t+x)(1+M_0)-2c}{(t+x)(1+M_0)}} \tag{7}$$

and their argument ψ by

$$\psi=\arcsin\sqrt{\frac{x+M_0t}{c}} \tag{8}$$

Equations (6a) and (6b) give the loading over the complete wing section for values of t less than or equal to $2c/(1-M_0^2)$. Since M_0t/c equals U_0t'/c, the number of chord lengths traveled, these equations represent the exact linearized solution for the section load distribution during the time required for the wing to travel $2M_0/(1-M_0^2)$ chord lengths after reaching the gust front. Hence, for a Mach number equal to 0.8, equations (6) establish the gust response during the first 4.44 chord lengths of travel after the gust penetration. Figure 4 shows the variation of gust loading $\Delta p/qg$ throughout this interval and also, for comparative purposes, the indicial load variation $\Delta p/q\alpha$ for the first four chord lengths of travel.

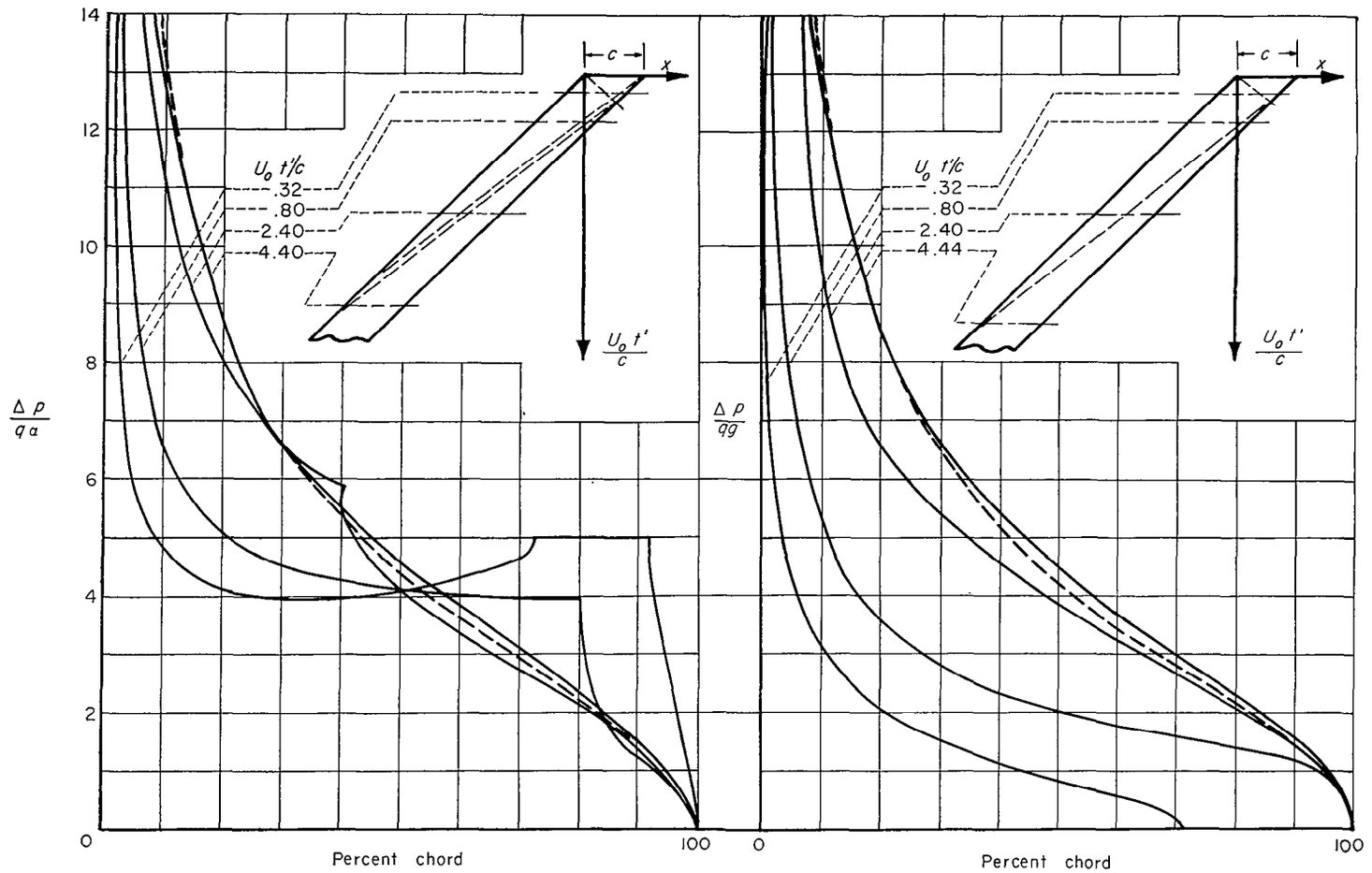

FIGURE 4.—Gust and indicial loading on two-dimensional wing. $M_0=0.8$.

The dashed curves in figure 4 represent the final steady-state load distribution adjusted so as to give the same total lift as the exact solutions for the gust and indicial cases at U_0t'/c equal to 4.44 and 4, respectively. Thus, to the degree of accuracy indicated in figure 4, the gust and indicial loadings at $M_0=0.8$ can be approximated for larger values of U_0t'/c by the expressions

$$\frac{\Delta p}{qg}=\frac{4}{\sqrt{1-M_0^2}}\sqrt{\frac{c-x}{x}}\left[\frac{c_{l_g}(U_0t'/c)}{c_{l_g}(\infty)}\right];\ \frac{2M_0}{1-M_0^2}<\frac{U_0t'}{c} \quad (9a)$$

and

$$\frac{\Delta p}{q\alpha}=\frac{4}{\sqrt{1-M_0^2}}\sqrt{\frac{c-x}{x}}\left[\frac{c_{l_\alpha}(U_0t'/c)}{c_{l_\alpha}(\infty)}\right];\ \frac{M_0}{1-M_0}<\frac{U_0t'}{c} \quad (9b)$$

The variation of c_{l_g} and c_{l_α} for values of U_0t'/c greater than 4 will be discussed presently.

For a Mach number equal to 0.5, equations (6) are sufficient to establish the gust response for only the first 1.33 chord lengths traveled. Further calculations were carried out and the exact loading was established for both the gust and indicial cases for values of U_0t'/c less than or equal to 2.33. These calculations were for the most part numerical and no simple closed expressions such as those presented in equations (6) were obtained. Figure 5 contains the results. Again, the dashed curves represent the final adjusted steady-state load distribution indicating that the gust and indicia loadings for $M_0=0.5$ can also be approximated for larger values of U_0t'/c by the equations (9).

Section lift.—When integrated across the chord at a fixed time, the loadings shown in figures 4 and 5 give the variation of the lifting force on the wing section during the early portion of the response. In the interval $0\leq U_0t'/c\leq M_0/(1+M_0)$ equation (6a) integrates to give

$$\frac{c_l}{w_0/U_0}=c_{l_g}=\left(\frac{U_0t'}{c}\right)\frac{4}{\sqrt{M_0}} \quad (10)$$

In the interval $M_0/(1+M_0)\leq U_0t'/c\leq 2M_0/(1-M_0^2)$ the expression for the loading is too complicated to integrate analytically and the section lift was calculated by numerical methods. The results, together with those for c_{l_α} (taken from ref. 15), are given in figure 6. Since, as time goes on, c_{l_g} must approach c_{l_α}, the curve for the gust response was simply faired into the curve for the indicial response in the manner shown by the dashed lines. Finally, for values of U_0t'/c greater than 10, the following equations, taken from reference 1, can be used:

For $M_0=0.5$,

$$c_{l_g}\approx c_{l_\alpha}\approx\frac{2\pi}{\sqrt{1-M_0^2}}\left\{1-\frac{1.333}{5+2(U_0t'/c)}-\frac{44.218}{[5+2(U_0t'/c)]^2}\right\} \quad (11a)$$

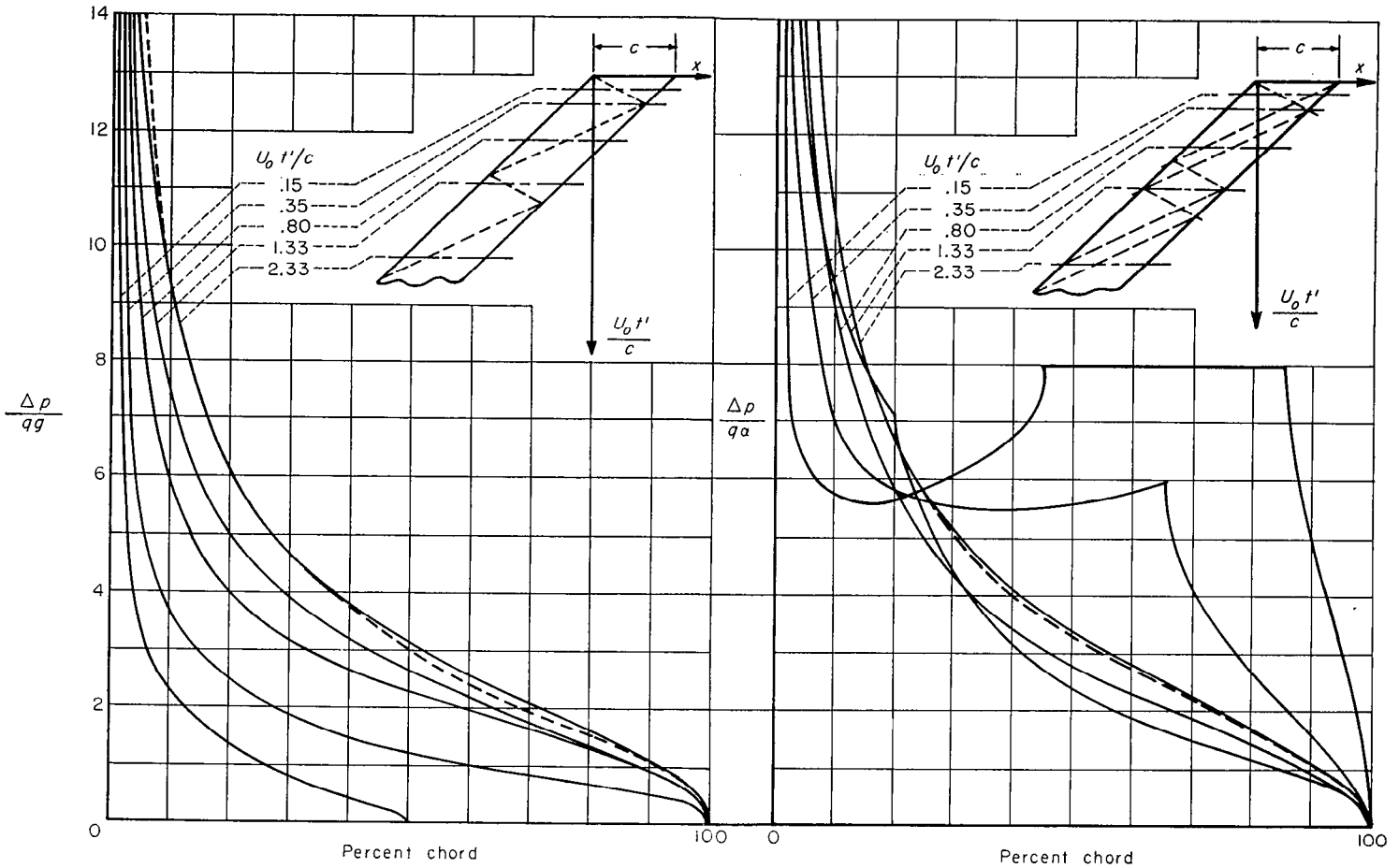

FIGURE 5.—Gust and indicial loading on two-dimensional wing. $M_0=0.5$.

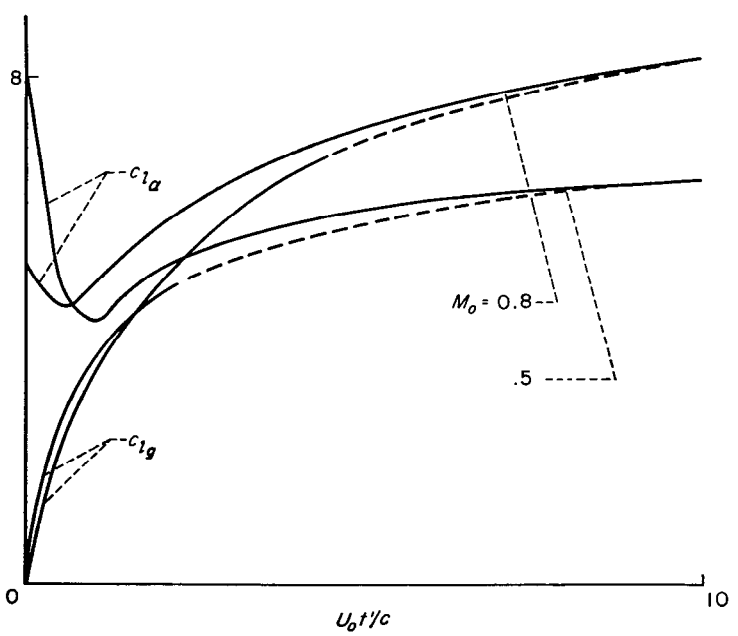

FIGURE 6.—Initial variations of c_{l_α} and c_{l_g}.

For $M_0=0.8$,

$$c_{l_g} \approx c_{l_\alpha} \approx \frac{2\pi}{\sqrt{1-M_0^2}}\left\{1-\frac{1.736}{11+1.25(U_0t'/c)}-\frac{70.83}{[11+1.25(U_0t'/c)]^2}\right\} \tag{11b}$$

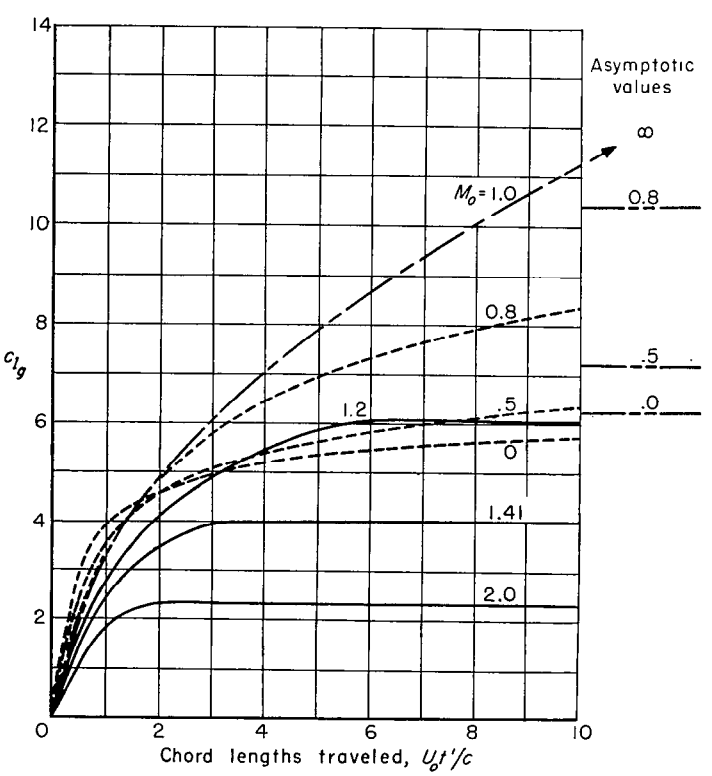

(a) Two-dimensional wing for several Mach numbers.

FIGURE 7.—Response of restrained wing to unit sharp-edged gust.

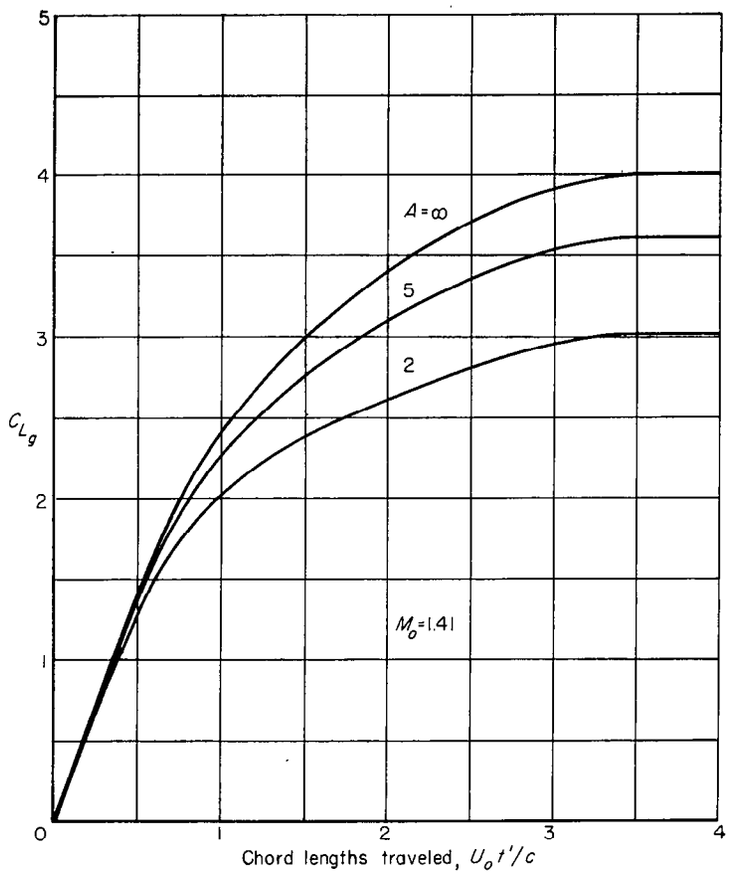

(b) Rectangular wings of aspect ratios 2, 5, and ∞.
FIGURE 7.—Concluded.

The final curves (determined from the previous analysis and aforementioned references) for c_{l_g}, the section lift coefficient developed on a restrained wing entering a sharp-edged gust, are shown in figure 7(a) for Mach numbers equal to 0, 0.5, 0.8, 1.0, 1.2, 1.41, and 2.0. Tabular values are given in tables I and II for Mach numbers equal to 0.5 and 0.8. The effect of aspect ratio at a Mach number equal to 1.41 is shown in figure 7(b).

TABLE I.—VALUES OF c_{l_α} AND c_{l_g} FOR $M_0=0.5$

U_0t'/c	$\sqrt{1-M_0^2}c_{l_\alpha}/2\pi$	$\sqrt{1-M_0^2}c_{l_g}/2\pi$
0	1.103	0
.1	.995	.081
.2	.882	.158
.3	.772	.236
.4	.691	.301
.5	.656	.347
.6	.634	.382
.7	.618	.413
.8	.604	.441
.9	.588	.438
1.0	.579	.488
1.1	.581	.509
1.2	.597	.526
1.3	.617	.545
1.4	.634	.560
1.5	.642	.573
1.6	.659	.586
1.7	.669	.598
1.8	.677	.609
1.9	.685	.619
2.0	.693	.629
2.5	.724	.673
3.0	.746	.704
3.5	.765	.727
4.0	.781	.746
4.5	.795	.764
5.0	.806	.779
5.5	.816	.793
6.0	.825	.806
6.5	.832	.815
7.0	.840	.826
7.5	.848	.835
8.0	.854	.845
9.0	.866	.862
10.0	.877	.877
∞	1.000	1.000

TABLE II.—VALUES OF c_{l_α} AND c_{l_g} FOR $M_0=0.8$

U_0t'/c	$\sqrt{1-M_0^2}c_{l_\alpha}/2\pi$	$\sqrt{1-M_0^2}c_{l_g}/2\pi$
0	0.478	0
.1	.466	.044
.2	.454	.085
.3	.442	.129
.4	.430	.170
.5	.423	.209
.6	.426	.234
.7	.433	.256
.8	.442	.276
.9	.451	.296
1.0	.461	.315
1.5	.507	.402
2.0	.546	.465
2.5	.581	.513
3.0	.610	.551
3.5	.632	.584
4.0	.652	.616
4.5	.670	.642
5.0	.687	.663
6.0	.714	.700
7.0	.738	.730
8.0	.760	.758
9.0	.779	.780
10.0	.798	.796
∞	1.000	1.000

RESPONSE OF AN UNRESTRAINED WING TO A SHARP-EDGED GUST

Given the indicial lift response C_{L_α} and the response for a restrained wing penetrating a sharp-edged gust C_{L_g}, one can use equation (3) to find the motion of an unrestrained wing entering a sharp-edged gust having a constant upward velocity w_0. As in reference 4, the lift on the unrestrained wing can be related to an infinite series of integrals involving C_{L_α} and C_{L_g}. First, set

$$\tau=\frac{U_0t'}{c}, \qquad \tau_1=\frac{U_0t_1'}{c}$$

$$-\frac{w}{U_0}=\alpha, \qquad \mu=\frac{2m}{\rho_0cS}$$

so that, by integrating equation (3) with respect to t', one finds

$$w=\frac{w_0}{\mu}\int_0^\tau C_{L_g}(\tau_1)d\tau_1+\frac{1}{\mu}\int_0^\tau C_{L_\alpha}(\tau-\tau_1)w(\tau_1)d\tau_1=0 \quad (12)$$

Then use the relation

$$\frac{C_L}{w_0/U_0}=(dw/d\tau)(\mu/w_0)$$

and iterate equation (12) using Liouville's method of successive substitutions. (See ref. 18.) This yields

$$\frac{C_L}{w_0/U_0}=C_{L_g}(\tau)-\frac{1}{\mu}\int_0^\tau C_{L_\alpha}(\tau-\tau_1)C_{L_g}(\tau_1)d\tau_1+$$

$$\frac{1}{\mu^2}\int_0^\tau C_{L_\alpha}(\tau-\tau_1)d\tau_1\int_0^{\tau_1}C_{L_\alpha}(\tau_1-\tau_2)C_{L_g}(\tau_2)d\tau_2-\ldots \quad (13)$$

Equation (13) converges uniformly [3] for all τ. By means

[3] The statement made in reference 4 on the convergence of this series is unnecessarily restrictive. Since the greatest values of C_{L_α} and C_{L_g} are $C_{L_\alpha}(\infty)$ and $C_{L_g}(\infty)$, the general term of the series does not exceed

$$\frac{1}{\mu^n}[C_{L_\alpha}(\infty)]^n C_{L_g}(\infty)\int_0^\tau d\tau_1\int_0^{\tau_1}d\tau_2\int_0^{\tau_2}d\tau_3\ldots\int_0^{\tau_{n-1}}d\tau_n$$

that is, does not exceed

$$\frac{1}{\mu^n}[C_{L_\alpha}(\infty)]^n C_{L_g}(\infty)\frac{1}{n!}\tau^n$$

and by the ratio test the series converges uniformly.

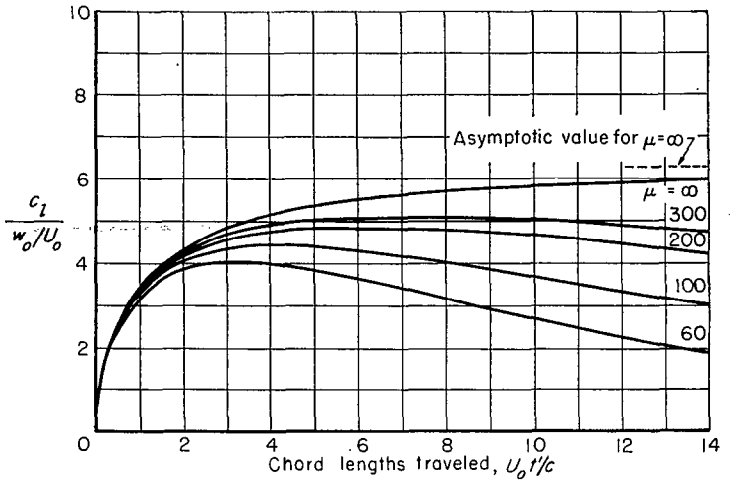

(a) $M_0=0$, $A=\infty$

FIGURE 8.—Response of unrestrained wing to a uniform, sharp-edged gust.

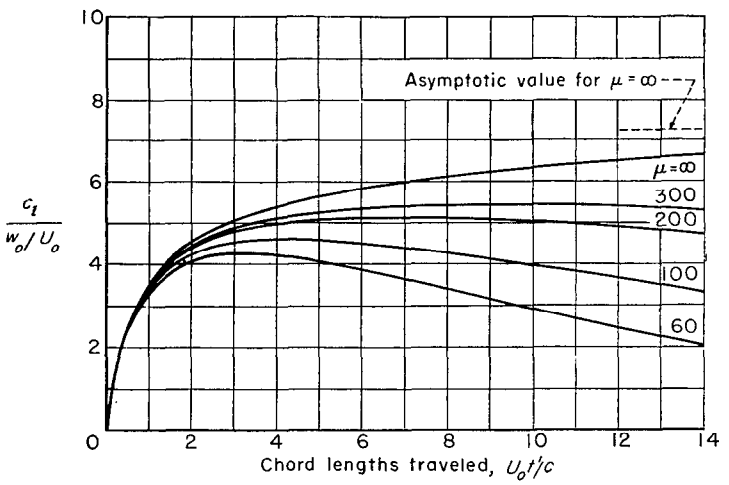

(b) $M_0=0.5$, $A=\infty$

FIGURE 8.—Continued.

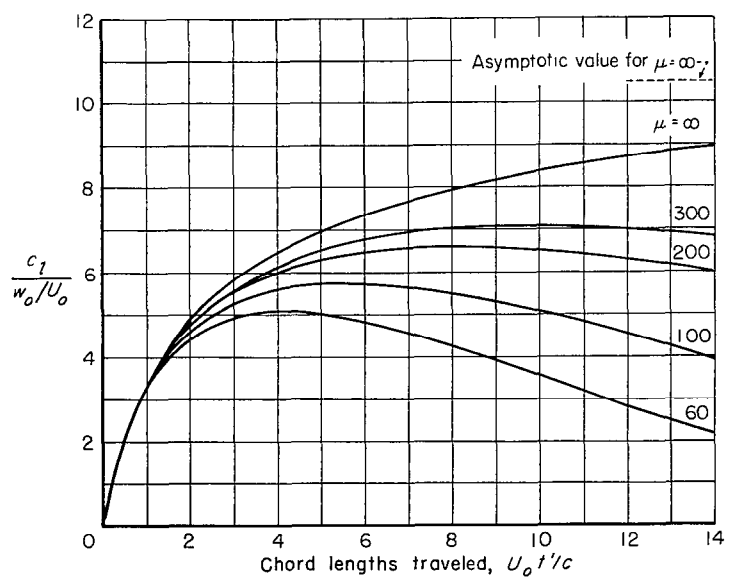

(c) $M_0=0.8$, $A=\infty$

FIGURE 8.—Continued.

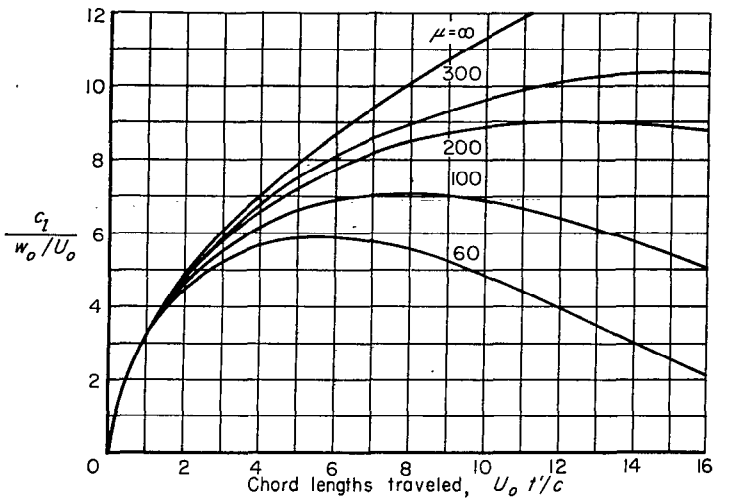

(d) $M_0=1.0$. $A=\infty$

FIGURE 8.—Continued.

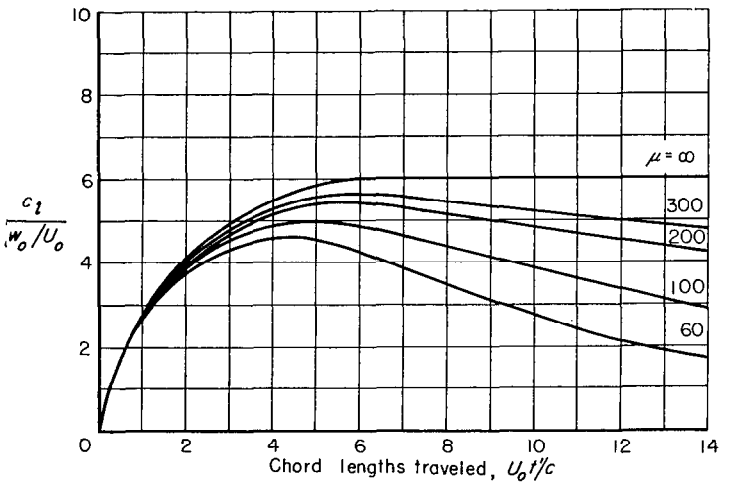

(e) $M_0=1.2$, $A=\infty$

FIGURE 8.—Continued.

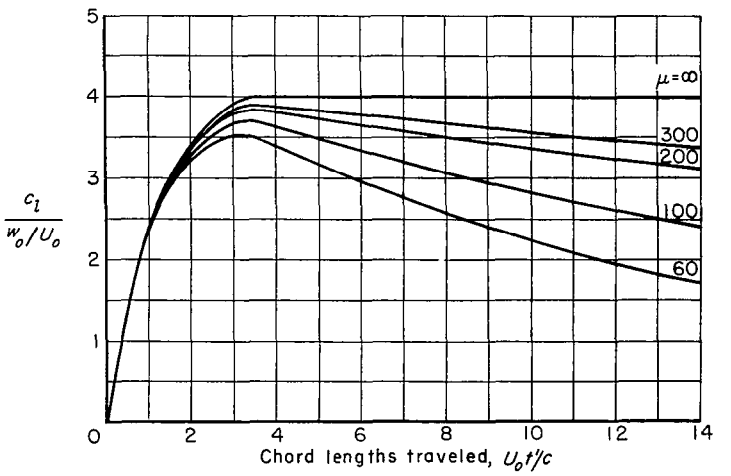

(f) $M_0=1.41$, $A=\infty$

FIGURE 8.—Continued.

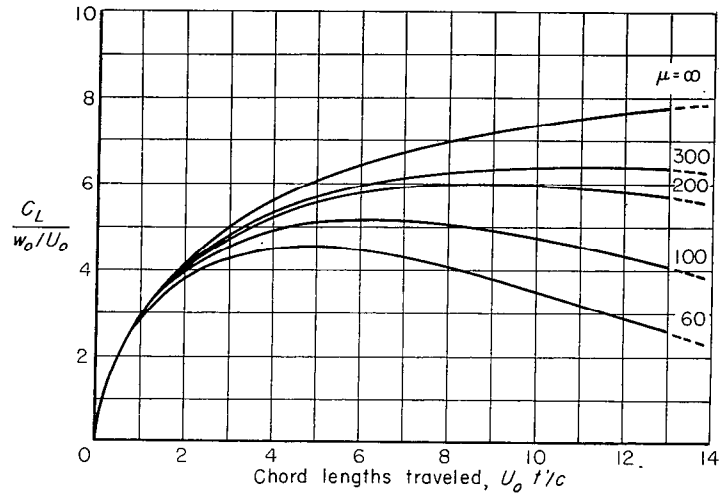

(g) $M_0=1.00$, $A=5$
FIGURE 8.—Continued.

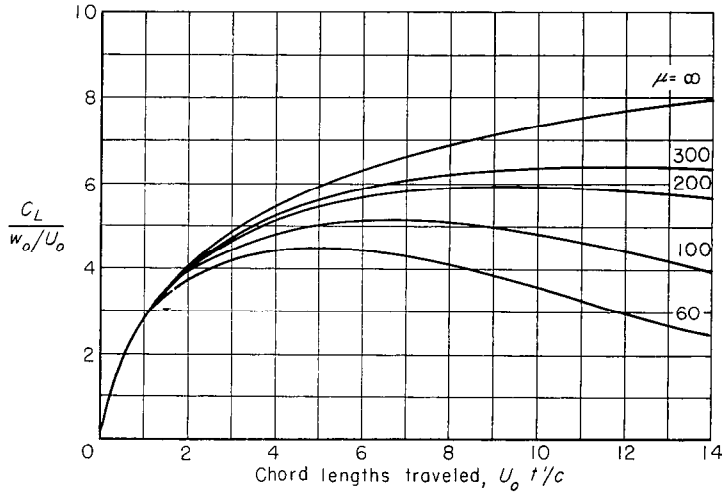

(h) $M_0=1.02$, $A=5$
FIGURE 8.—Continued.

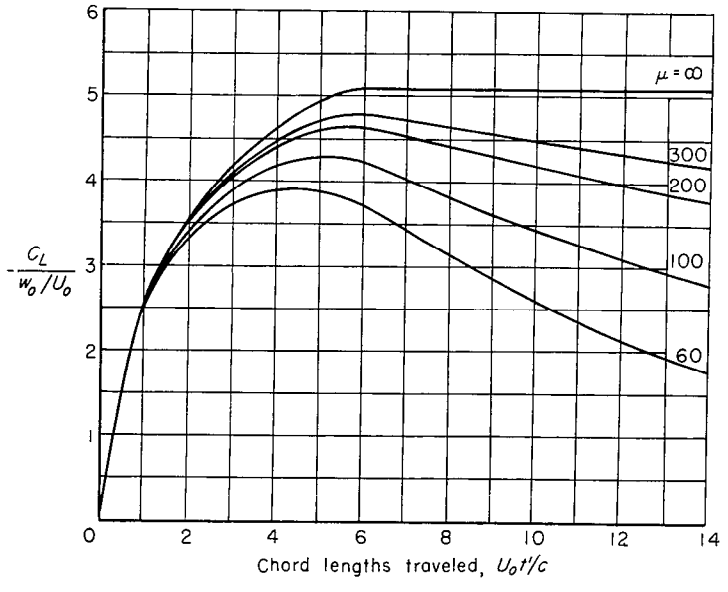

(i) $M_0=1.2$, $A=5$
FIGURE 8.—Continued.

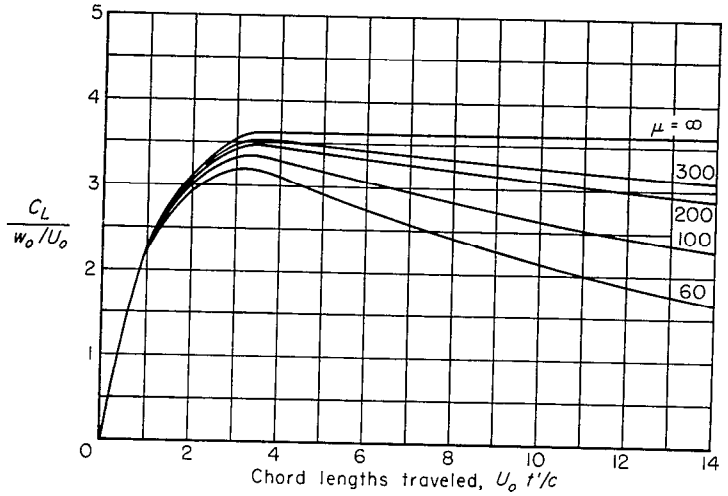

(j) $M_0=1.41$, $A=5$
FIGURE 8.—Continued.

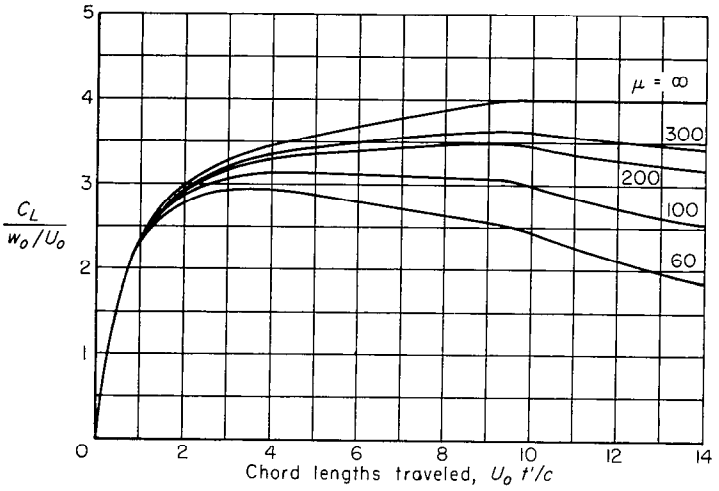

(k) $M_0=1.12$, $A=2$
FIGURE 8.—Continued.

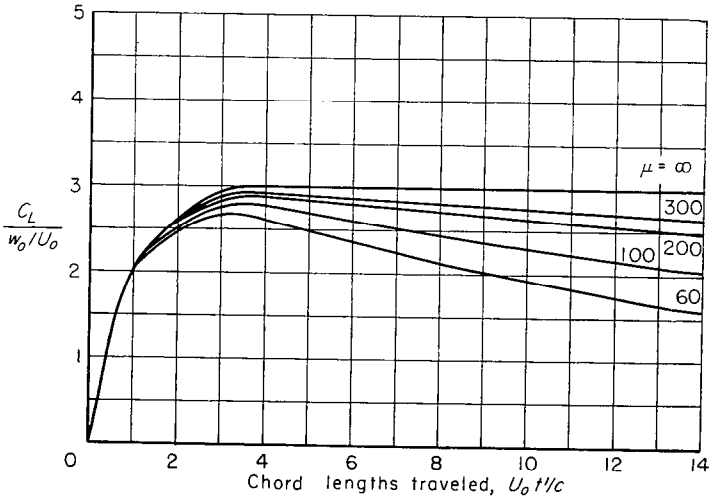

(l) $M_0=1.41$, $A=2$
FIGURE 8.—Concluded.

of it, $C_L/(w_0/U_0)$ and $c_l/(w_0/U_0)$, the total and section lift coefficients induced on unrestrained wings entering a sharp-edged gust, have been calculated and the results are shown in figure 8. Table III indicates the range of Mach numbers and aspect ratios for which calculations were made, the numbers in the chart referring to the individual figures in which the results are presented. It should be noted that results are given for a wing flying at $M_0=1$ and having a finite aspect ratio. Such cases can be calculated from the indicial and restrained gust responses presented in reference 5. These responses are still valid at $M_0=1$ for values of the time variable up to that for which the wave envelope induced by one side of the wing crosses the opposite side. A wing of aspect ratio 5 flying at the speed of sound travels 13 chord lengths during this time interval, and this is sufficient to establish the significant part of the response to a sharp-edged gust for $\mu \leq 300$.

TABLE III.—VALUES OF MACH NUMBER AND ASPECT RATIO FOR WHICH CALCULATIONS WERE CARRIED OUT

M_0 \ A	2	5	∞
0	.....	.....	8a
.5	.....	.....	8b
.8	.....	.....	8c
1.0	.....	8g	8d
1.02	.....	8h	.....
1.12	8k	.....	.....
1.20	.....	8i	8e
1.41	8l	8j	8f

The chart also shows that the gust response for the unrestrained wing was calculated at $M_0=0$ for an infinite-aspect-ratio wing (for comparative purposes) but not for finite-aspect-ratio wings. The gust response on both infinite- and finite-aspect-ratio wings in incompressible flow has been studied extensively by means of operational methods in references 12, 13, and 14. Where comparisons can be made, the results obtained in this report using equation (13) agree well with those given in the references mentioned.

RESPONSE OF UNRESTRAINED WING TO ARBITRARY GUST

The function $C_L/(w_0/U_0)$ presented in the previous section can be thought of as the indicial gust response for lift on an unrestrained wing. In this sense it is apparent that the lift on a wing penetrating a gust in which w is a function of the chord lengths traveled can be calculated by superposition and is represented by the integral

$$C_L=\frac{d}{d\tau}\int_0^\tau \frac{C_L(\tau_1)}{w_0/U_0}\frac{w(\tau-\tau_1)}{U_0}\,d\tau_1 \tag{14}$$

By means of equation (14), the lift induced on a wing moving at the constant speed U_0 and entering a gust, the vertical velocity of which starts at zero and increases linearly with distance of penetration, is simply the integral of $C_L/(w_0/U_0)$. Thus, representing the section lift coefficient developed by a wing entering a gust with a unit gradient by the symbol C_{L_s}, we can write

$$C_{L_s}(\tau)=\int_0^\tau \frac{C_L(\tau_1)}{w_0/U_0}\,d\tau_1 \tag{15}$$

If the wing flies into a gust with a triangular-shaped distribution of w, having its maximum intensity w_t a distance h chord lengths from the front, it follows at once that the resulting lift response $C_L/(w_t/U_0)$ is given by

$$\frac{C_L}{w_t/U_0}=\begin{cases}\frac{1}{h}\left[C_{L_s}(\tau)\right]; & 0\leq\tau\leq h\\ \frac{1}{h}\left[C_{L_s}(\tau)-2C_{L_s}(\tau-h)\right]; & h\leq\tau\leq 2h\\ \frac{1}{h}\left[C_{L_s}(\tau)-2C_{L_s}(\tau-h)+\right. & \\ \left. C_{L_s}(\tau-2h)\right]; & 2h\leq\tau\end{cases} \tag{16}$$

Examples of the various gust shapes and the responses in lift and vertical motion of wings penetrating them are shown in figure 9.

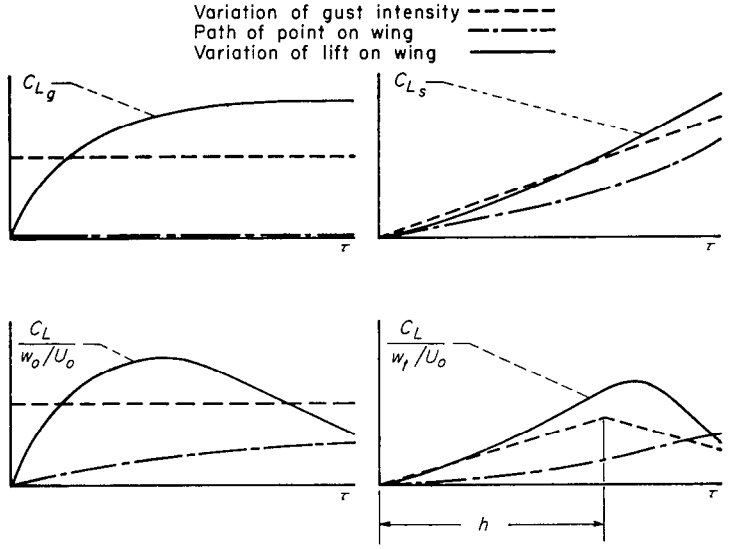

FIGURE 9.—Gust shapes and responses.

MAXIMUM LIFT DUE TO GUST PENETRATION

SHARP-EDGED GUST

Consider the maximum increase in lift caused by the entry of the wing into a sharp-edged gust. This increment is given for the range of Mach numbers, aspect ratios, and wing-air density ratios shown in table III by the maximum values of $C_L/(w_0/U_0)$ and $c_l/(w_0/U_0)$ on the curves shown in figure 8.

First, let us consider wings of infinite aspect ratio. For such wings the variation of the maximum gust-induced lift coefficient with Mach number is shown in figure 10, and a cross plot in which M_0 instead of μ is held constant is presented in figure 11. The values for $\mu=\infty$ are the steady-state values given by the simple equations

$$\left(\frac{c_l}{w_0/U_0}\right)_{max}=\begin{cases}2\pi/\sqrt{1-M_0^2}; & M_0<1\\ 4/\sqrt{M_0^2-1}; & M_0>1\end{cases}$$

The difference between the lift increment on a restrained wing and that on one with a finite value of μ is seen to be most pronounced at the high subsonic Mach numbers. Notice, for example, that the percentage increase in $[c_l/(w_0/U_0)]_{max}$ found by increasing M_0 from 0 to 0.8 is 67 for $\mu=\infty$

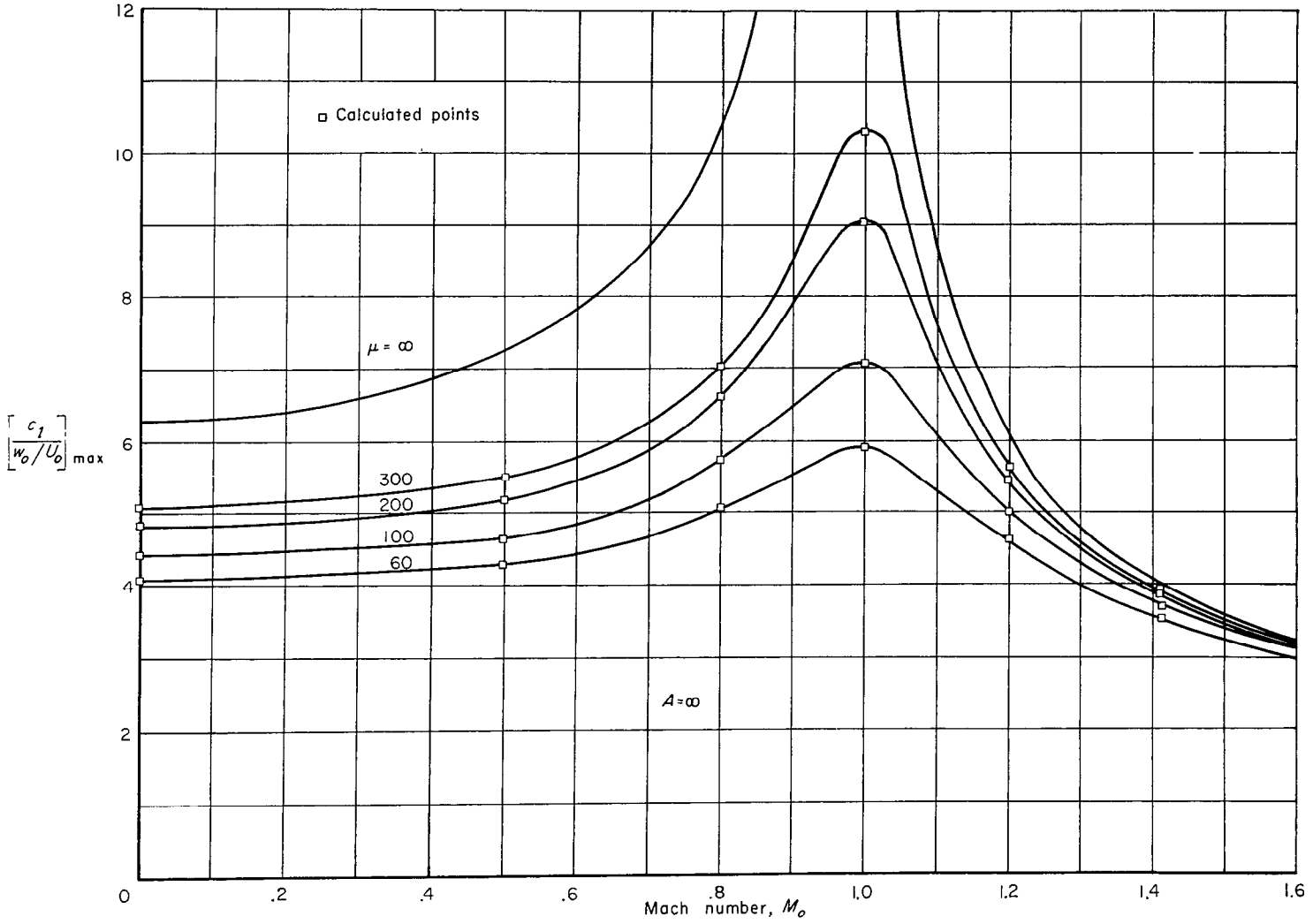

FIGURE 10.—Maximum increment of lift induced on a two-dimensional wing entering a uniform sharp-edged gust.

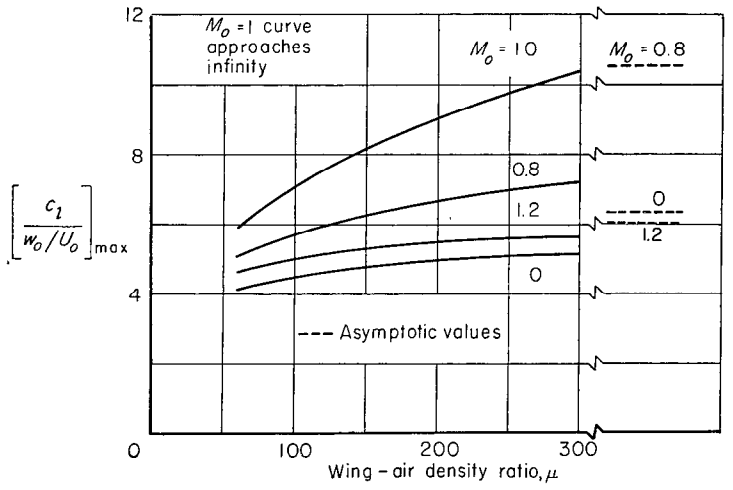

FIGURE 11.—Maximum gust-induced lift on two-dimensional wings.

(Prandtl Glauert rule) but only 37 for $\mu=200$. Table IV indicates the relative increase in $[c_l/(w_0/U_0)]_{max}$ caused by compressibility for three different values of the wing-air density ratio.

TABLE IV.—PERCENT INCREASE IN $(c_l)_{max}$ RELATIVE TO ITS VALUE AT $M_0=0$.

M_0 \ μ	∞	300	200
0	0	0	0
.8	67	39	37
1.0	∞	103	88
1.2	−4	10	12

Consider next the effect of aspect ratio on the maximum lift increment induced on a rectangular wing penetrating a sharp-edged gust. When $\mu=\infty$ this increment is again given by the steady-state value of the lift-curve slope and is presented for $A=\infty$, 5, and 2, in figure 12. These steady-state values are taken from the numerous studies made of lifting surfaces traveling at subsonic and supersonic speeds. On the supersonic side, for cases in which $A\sqrt{M_0^2-1}\geq 1$, the equation (see, e. g., ref. 19)

$$\left(\frac{C_L}{w_0/U_0}\right)_{max}=\frac{4}{\sqrt{M_0^2-1}}\left(1-\frac{1}{2A\sqrt{M_0^2-1}}\right)$$

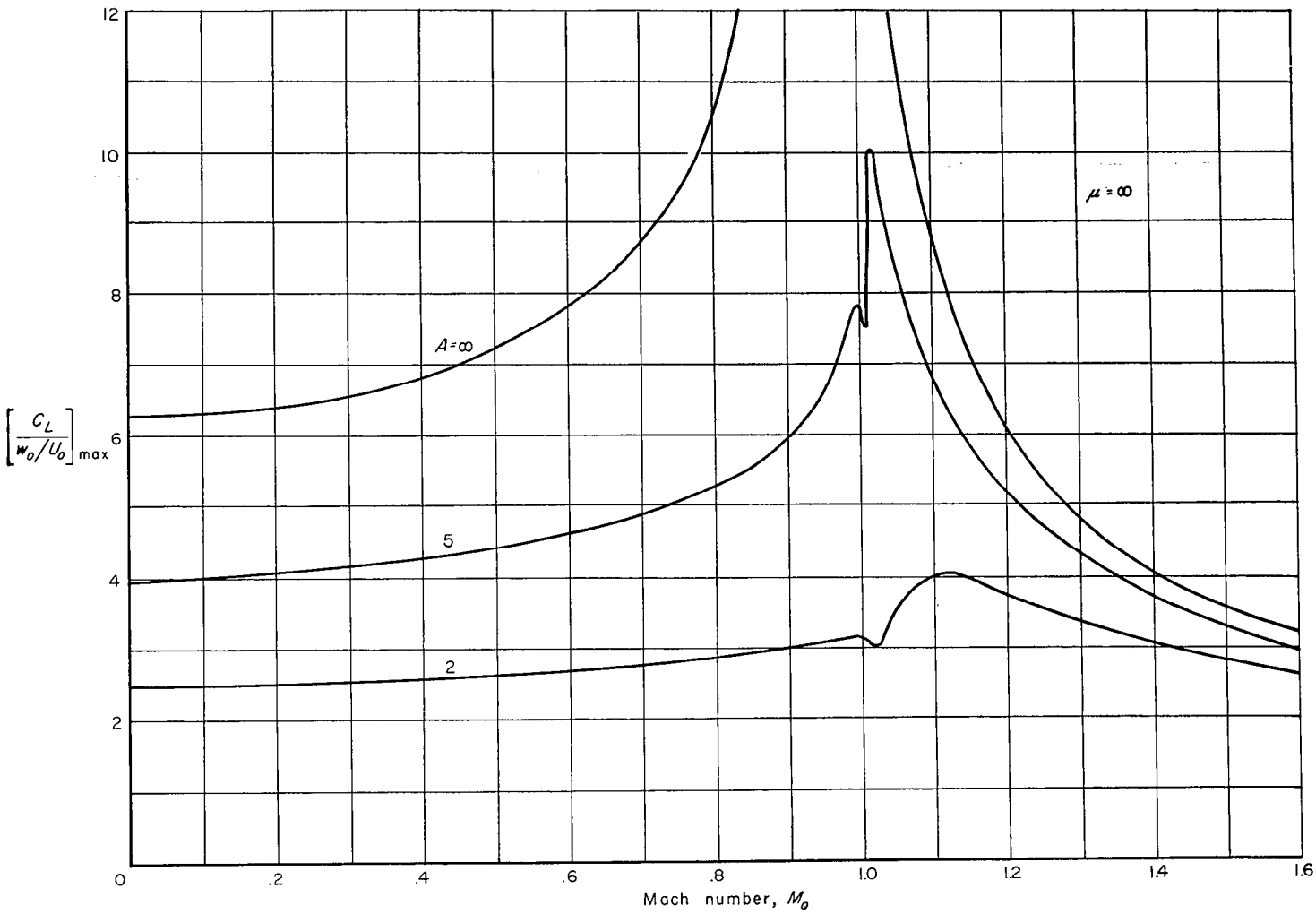

FIGURE 12.—Maximum increment of lift induced on restrained rectangular wing entering a uniform sharp-edged gust.

applies and, for cases in which $1 \geq A\sqrt{M_0^2-1} \geq 0$, the curves in reference 20 were used. On the subsonic side the portions of the curves in the range $0 \leq A\sqrt{1-M_0^2} \leq 2$ were again taken from reference 20. The results in references 19 and 20 are sufficient to cover the entire Mach number range for the $A=2$ wing. For the $A=5$ wing the values on the subsonic side outside the range $0 \leq A\sqrt{1-M_0^2} \leq 2$ were taken from a curve [4] that was compiled from a large number of solutions for lifting surfaces traveling at subsonic speeds.

The values of $[C_L/(w_0/U_0)]_{max}$ for rectangular wings traveling at supersonic speeds, given in figure 8, and the incompressible-flow solutions, given in references 12, 13, and 14, were used to prepare the curves in figure 13. The dashed lines between the Mach numbers of 0 and that for which $A\sqrt{M_0^2-1}=1$ are interpolated, the two-dimensional results presented in figure 10 lending credence to the validity of the interpolation. Figure 14 presents the aspect-ratio effect on $[C_L/(w_0/U_0)]_{max}$ at $M_0=1$.

It should be noted that in the vicinity of $M_0=1$, the curves for which $A=\infty$, $\mu=\infty$ (figs. 10 and 12), and probably also those for which $A=5$, $\mu=\infty$ (figs. 12 and 13 (a)), are not valid representations of the gust-induced lift on actual wings flying at these speeds, although they do represent solutions to equation (4) consistent with the boundary conditions previously discussed. For the two cases mentioned, the assumptions on which equation (4) is based are violated. These assumptions are more closely approached, however, as the wing-air density ratio and the aspect ratio decrease. Hence, for lower values of A and μ the solutions given herein for wings traveling in the transonic speed range have justification on a physical as well as a mathematical basis.

[4] The curve was taken from an article prepared by Robert T. Jones and Doris Cohen for the forthcoming series on High-Speed Aerodynamics and Jet Propulsion, Princeton University Press.

TRIANGULAR GUST

The maximum increase in lift on a two-dimensional wing passing through a triangular gust having its maximum intensity 12 chord lengths from its front is shown in figure 15. For the lower values of μ, the variation of $[c_l/(w_l/U_0)]_{max}$ with Mach number is similar to that calculated for the sharp-edged gust and shown in figure 10. As μ increases, however, a comparison of the results shown in these two figures indicates the importance of the assumed gust shape in estimating the maximum gust-induced lift. Table V shows the difference in the compressibility effect obtained for the sharp-edged and triangular (12 chord lengths to apex) gusts.

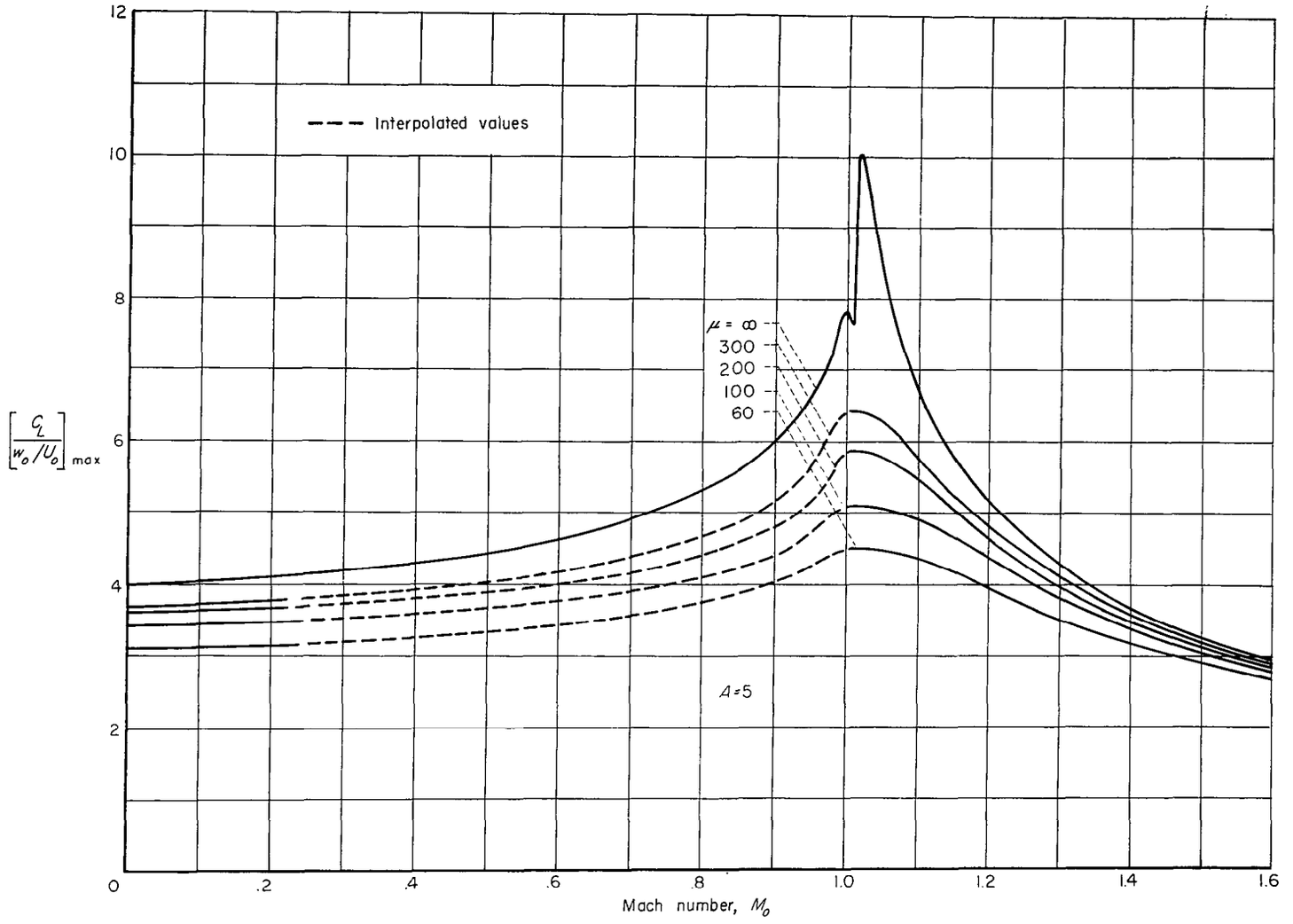

(a) $A=5$

FIGURE 13.—Maximum increment of lift induced on a rectangular wing entering a uniform sharp-edged gust.

TABLE V.—RATIO OF THE VALUE OF $(C_L)_{max}$ AT $M_0=0.8$ AND 1.0 TO ITS VALUE AT $M_0=0$.

Gust type / μ	$M_0=0.8$		$M_0=1.0$	
	Sharp edge	Tri-angle	Sharp edge	Tri-angle
60	1.24	1.24	1.44	1.51
100	1.29	1.29	1.59	1.58
200	1.37	1.33	1.88	1.67
300	1.39	1.34	2.03	1.70
∞	1.66	1.38	∞	1.85

Figure 16 presents the aspect-ratio effect on the maximum lift response for rectangular wings penetrating triangular-shaped gusts. The values at $M_0=0$ were calculated from the results given in reference 12 and again the dashed lines represent an interpolation.

CONCLUDING REMARKS

Results are presented for the lift developed by a restrained two-dimensional wing flying at a Mach number equal to 0.5 or 0.8 and penetrating a sharp-edged gust. Similar results are reviewed for Mach numbers equal to 0, 1.0, 1.2, 1.41, and 2.

A method is given whereby the lift can be estimated (neglecting the effects of airplane pitching and wing bending) for unrestrained rectangular wings in the aspect-ratio range 2 to ∞, flying in the Mach number range 0 to 2, and penetrating gusts of arbitrary structure. Specific results are given for sharp-edged and triangular-shaped gusts.

In general, given variations in the wing aspect ratio, the wing-air density ratio, and the gust shape have their maximum effect on the gust lift when the wing is flying at a high subsonic speed.

AMES AERONAUTICAL LABORATORY
NATIONAL ADVISORY COMMITTEE FOR AERONAUTICS
MOFFETT FIELD, CALIF., *Feb. 3, 1953.*

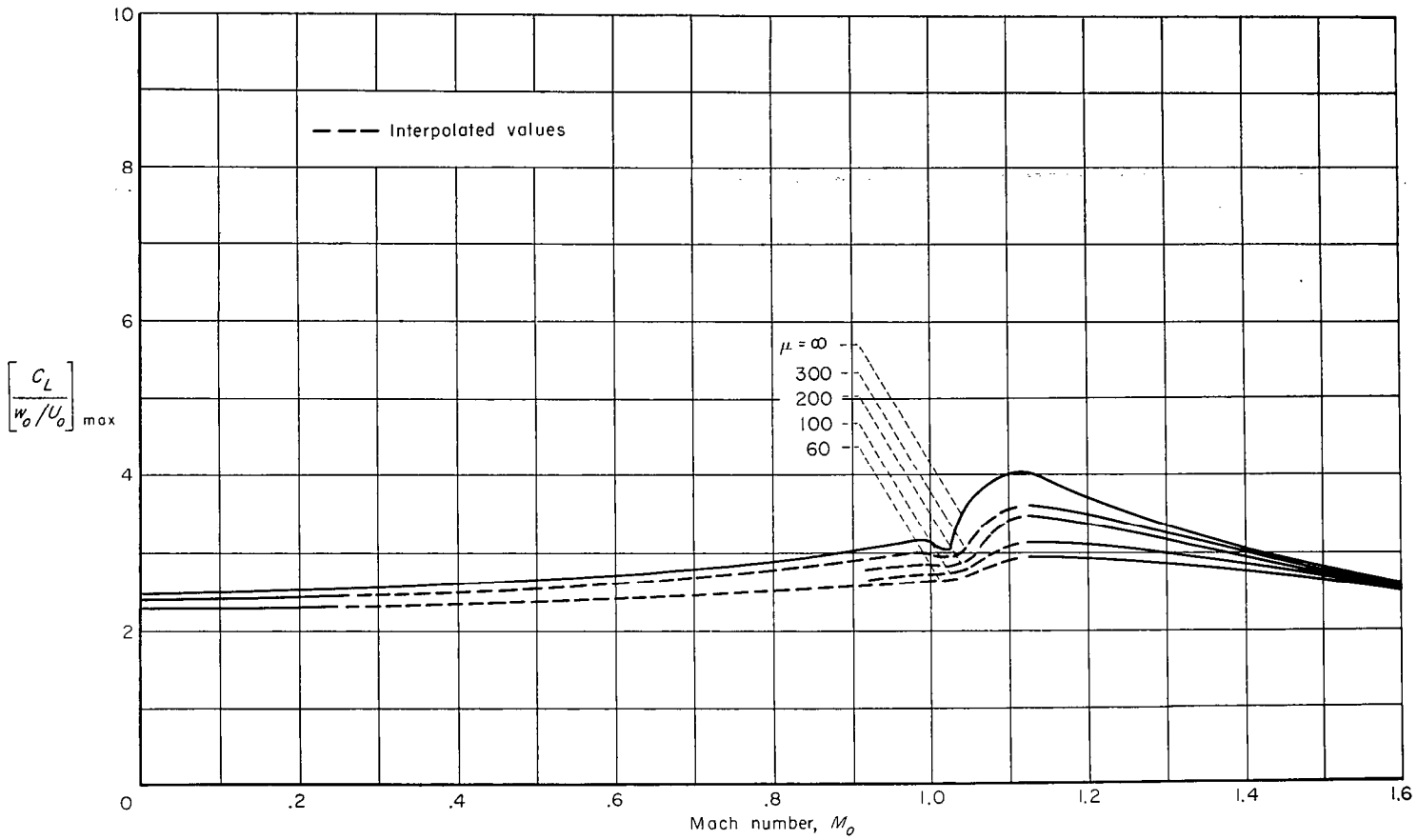

(b) $A=2$

FIGURE 13.—Concluded.

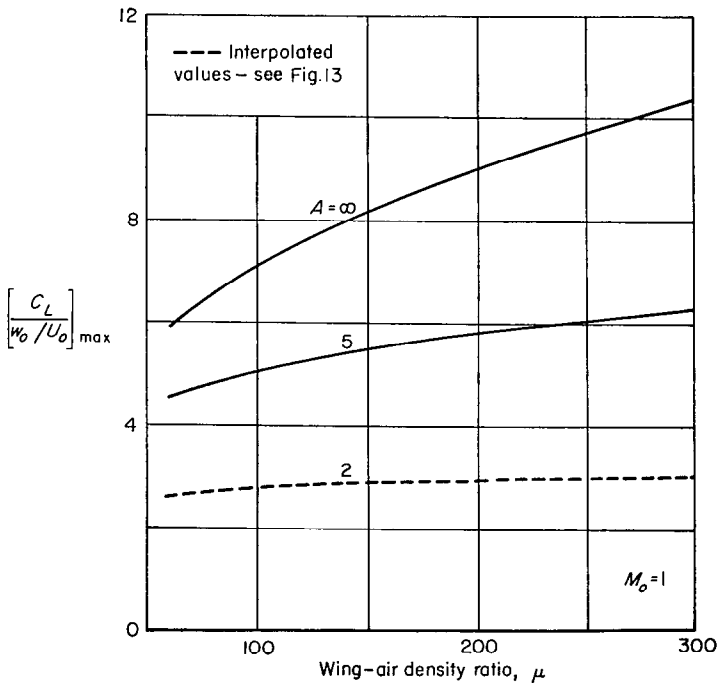

FIGURE 14.—Maximum gust-induced lift on rectangular wings.

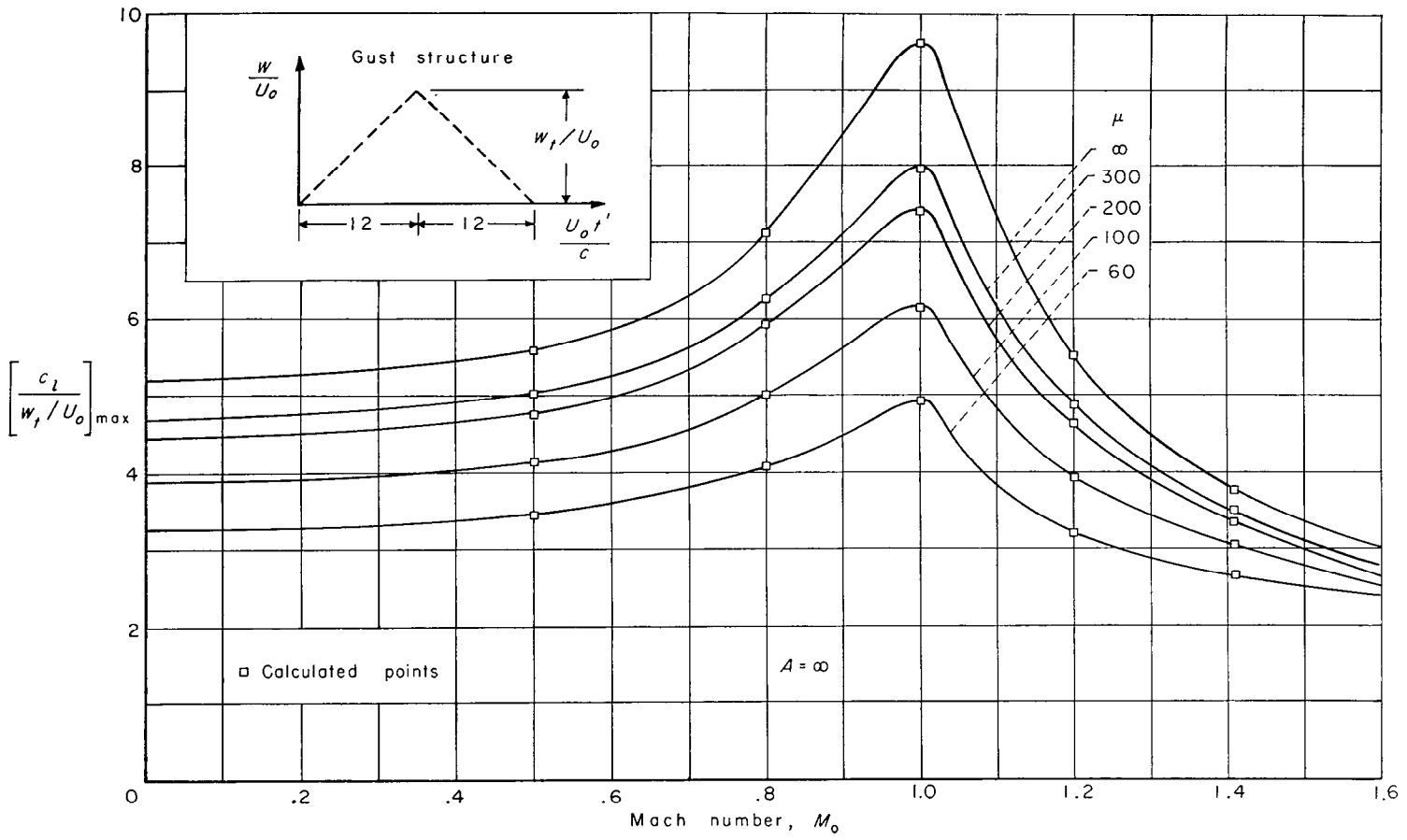

FIGURE 15.—Maximum increment of lift induced on a two-dimensional wing entering a triangular gust having its apex 12 chord lengths from the front.

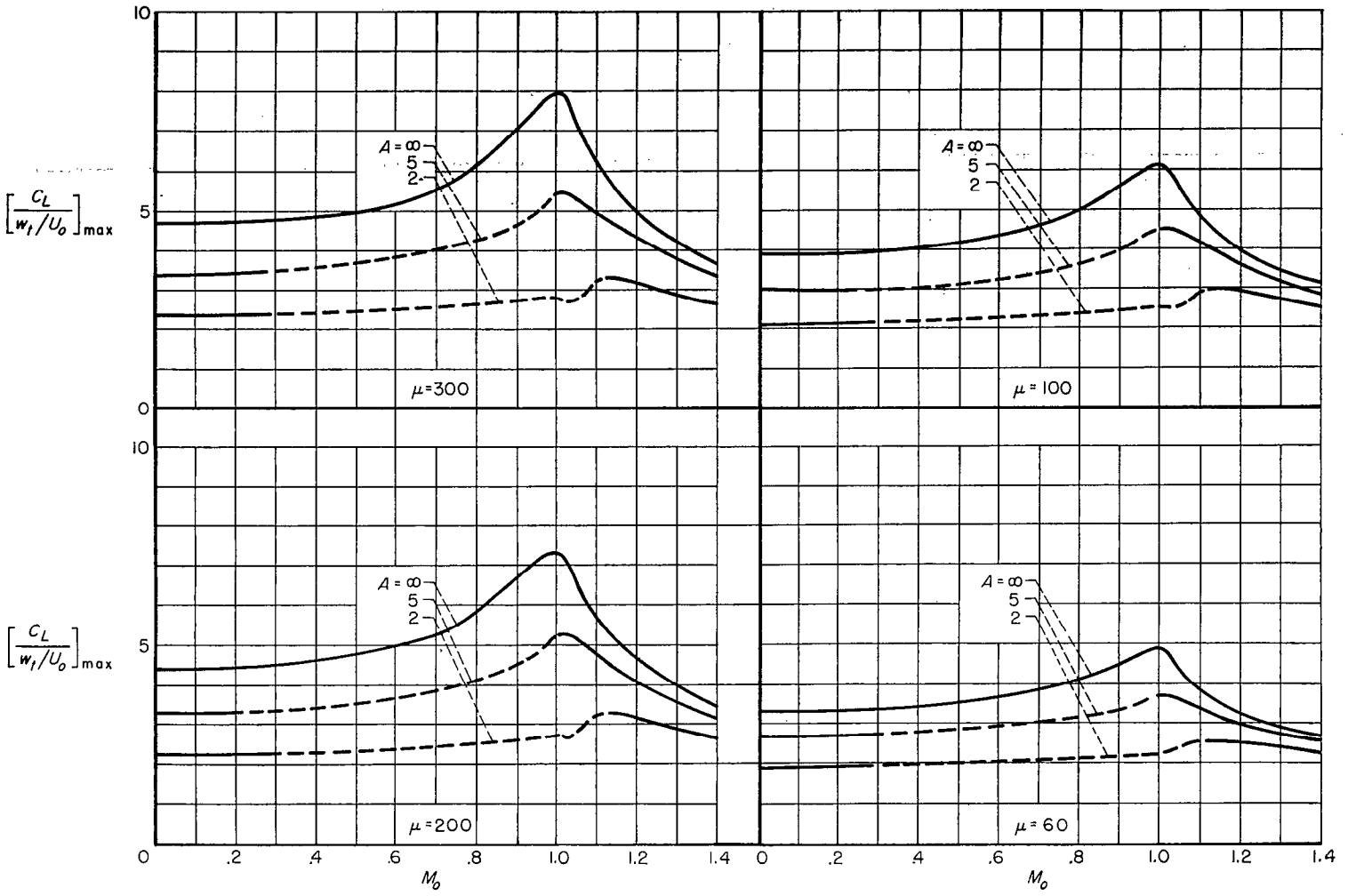

FIGURE 16.—Maximum increment of lift induced on a rectangular wing entering a triangular gust having its apex 12 chord lengths from the front

APPENDIX

LIST OF SYMBOLS

A	aspect ratio
a_0	speed of sound
c	chord length
C_L	wing lift coefficient, $\frac{L}{qS}$
c_l	section lift coefficient, $\frac{L}{qc}$
E	complete elliptic integral of second kind with modulus k
$E'(\psi)$	incomplete elliptic integral of second kind with modulus k' and argument ψ
$F'(\psi)$	incomplete elliptic integral of first kind with modulus k' and argument ψ
g	$\frac{w_0}{U_0}$
h	number of chord lengths from front to apex of triangular gust
K	complete elliptic integral of first kind with modulus k
k	modulus of elliptic integrals (See eq. (7).)
k'	$\sqrt{1-k^2}$
L	lift on wing
M_0	Mach number at which wing is traveling
m	mass of wing
$\frac{\Delta p}{q}$	loading coefficient, pressure on lower wing surface minus pressure on upper wing surface divided by dynamic pressure
q	dynamic pressure, $\frac{1}{2}\rho_0 U_0^2$
S	wing area
t'	time
t	$a_0 t'$
U_0	horizontal velocity of wing
w	vertical velocity of wing
$w_a(t')$	velocity of arbitrary gust
w_0	velocity of uniform, sharp-edged gust
w_t	maximum velocity of triangular gust
x, y, z	Cartesian coordinates fixed with reference to still air at infinity, z positive upward, y parallel to wing leading edge, negative x direction corresponding to direction of wing motion
α	wing angle of attack
μ	wing-air density ratio, $\frac{2m}{\rho_0 cS}$ in analysis of complete wing, $\frac{2m}{\rho_0 c^2}$ in analysis of wing section
ρ_0	air density
τ	chord lengths traveled by wing, $\frac{U_0 t'}{c}$
ϕ	perturbation velocity potential
ψ	argument of elliptic integrals (See eq. (8).)

Subscripts:

g	response of restrained wing to unit, sharp-edged gust
s	response to gust with unit velocity gradient
α	indicial response on sinking wing

REFERENCES

1. Miles, John W.: Transient Loading of Airfoils at Supersonic Speeds. Jour. Aero. Sci., vol. 15, no. 10, Oct. 1948, p. 592.
2. Strang, W. J.: A Physical Theory of Supersonic Aerofoils in Unsteady Flow. Proc. Roy. Soc., London, vol. 195, series A, no. 1041, 1948, pp. 245–264.
3. Biot, M. A.: Loads on a Supersonic Wing Striking a Sharp-Edged Gust. Jour. Aero. Sci., vol. 16, no. 5, May 1949, p. 296.
4. Heaslet, Max. A., and Lomax, Harvard: Two-Dimensional Unsteady Lift Problems in Supersonic Flight. NACA Rep. 945, 1949. (Supersedes NACA TN 1621).
5. Miles, John W.: Transient Loading of Supersonic Rectangular Airfoils. Jour. Aero. Sci., vol. 17, no. 10, Oct. 1950, p. 647.
6. Goodman, Theodore R.: Aerodynamics of a Supersonic Rectangular Wing Striking a Sharp-Edged Gust. Cornell Aeronautical Lab. Rep. No. AF–723–A–1, Sept. 1950.
7. Miles, John W.: Transient Loading of Wide Delta Airfoils at Supersonic Speeds. NAVORD. Rep. 1235, 1950.
8. Strang, W. J., Transient Lift of Three-Dimensional Purely Supersonic Wings. Proc. Roy. Soc., London, vol. 202, series A, no 1068, 1950, p. 54.
9. Wagner, Herbert: Uber die Entstehung des dynamischen Auftriebes von Tragflügeln. Z.F.a.M.M., Bd. 5, Heft 1, Feb. 1925, S. 17–35.
10. Kussner, Hans Georg: Stresses Produced in Airplane Wings by Gusts. NACA TM 654, 1932.
11. Von Kármán, Th., and Sears, W. R.: Airfoil Theory for Non-Uniform Motion. Jour. Aero. Sci., vol. 5, no. 10, Aug. 1938, p. 379.
12. Jones, Robert T.: The Unsteady Lift of a Wing of Finite Aspect Ratio. NACA Rep. 681, 1940.
13. Zbrozek, J.: Gust Alleviation Factor. Rep. No. Aero. 2421, R.A.E. (British), May 1951.
14. Bisplinghoff, R. L., Isakson, G., and O'Brien, T. F.: Gust Loads on Rigid Airplanes With Pitching Neglected. Jour. Aero. Sci., vol. 18, no. 1, Jan. 1951, p. 33.
15. Lomax, Harvard, Heaslet, Max. A., Fuller, Franklyn B., and Sluder, Loma: Two- and Three-Dimensional Unsteady Lift Problems in High-Speed Flight. NACA Rep. 1077, 1952.
16. Sears, William R.: Operational Methods in the Theory of Airfoils in Nonuniform Motion. J. Franklin Institute, vol. 230, July 1940, p. 95.
17. Heaslet, Max. A., and Spreiter, John R.: Reciprocity Relations in Aerodynamics. NACA Rep. 1119, 1953. (Supersedes NACA TN 2700)
18. Whittaker, E. T., and Watson, G. N.: A Course of Modern Analysis. 4th ed., Cambridge University Press (England), 1940, p. 221.
19. Heaslet, Max. A., Lomax, Harvard, and Jones, Arthur L.: Volterra's Solution of the Wave Equation as Applied to Three-Dimensional Supersonic Airfoil Problems. NACA Rep. 889, 1947. (Supersedes NACA TN 1412)
20. Lomax, Harvard, and Sluder, Loma: Chordwise and Compressibility Corrections to Slender-Wing Theory. NACA Rep. 1105, 1952. (Supersedes NACA TN 2295)

U. S. GOVERNMENT PRINTING OFFICE: 1954